Article

A cortical circuit for abrupt visual learning in the primate brain

Bennett A. Csorba[1,3,*], Matthew R. Krause[1], Theodoros P. Zanos[2], and Christopher C. Pack[1]
[1] Montreal Neurological Institute, McGill University, Montreal, QC H3A 2B4, Canada
[2] Feinstein Institute for Medical Research, Manhasset, NY 11030, USA
[3] Lead Contact
*Correspondence: bennett.csorba@mail.mcgill.ca

Summary

Visual cortical plasticity declines sharply after the critical period, and yet we easily learn to recognize new faces and places throughout our lives. Such learning is often characterized by a "moment of insight", an abrupt and dramatic improvement in recognition. We studied the brain mechanisms that support this kind of learning, using a behavioral task in which non-human primates rapidly learned to recognize visual images and to associate them with particular responses. Simultaneous recordings from the inferotemporal and prefrontal cortices revealed a transient synchronization of neural activity between these two areas that peaked around the moment of insight. This synchronization was strongest between inferotemporal sites that encoded images and prefrontal sites that encoded rewards. Moreover, its magnitude built up gradually with successive image exposures, suggesting that abrupt learning is the culmination of a search for informative visual signals within a circuit that links sensory information to task demands.

Introduction

In adults, visual learning often requires prolonged training. Even for simple tasks, such as discriminating the orientation of a line, behavioral changes often emerge after days or weeks of practice (Watanabe & Sasaki, 2015). For more complex tasks, such as the detection of anomalies in medical images, efficient performance requires months or years of training (Reingold & Sheridan, 2011; Laamerad, et al., 2020). Neurophysiological studies have similarly revealed that the adult visual cortex often changes very slowly, if at all, in response to experience (Yang & Maunsell, 2004; Ghose & Maunsell, 2002; Schoups, et al., 2001).

At the same time, it is clear that adults are capable of rapid visual learning under the right circumstances (Rubin, et al., 1997; Walsh & Booth, 1997; Ahissar & Hochstein, 1997). Indeed, this would seem to be necessary for natural visual experience, which does not always afford the opportunity for hundreds of exposures to novel stimuli. Consequently, it has been argued that observations of gradual learning are due to the design of laboratory experiments (Ahissar & Hochstein, 1997; Rubin, et al., 2002) or to the analysis of the resulting data (Gallistel, et al., 2004).

In the limit, rapid learning can occur following a single exposure to a stimulus (Brady, et al., 2008; Shepard, 1967; Standing, 1973; Mitchell, 2006), but more often it occurs *abruptly*, after a series of unsuccessful attempts at a task (Rubin, et al., 1997; Ahissar & Hochstein, 1997). Hebb (1949) argued that this kind of "insight" entails a strengthening of connections between groups of neurons that are synchronously active when the task is successfully performed. In support of this hypothesis, EEG studies have found increased synchronization between cortical regions during rapid learning (Miltner, et al., 1999). However, other studies have suggested that rapid learning could result from local changes in neural selectivity (Tovee, et al., 1996; Yao, et al., 2007). At present, the rules that govern visual learning under naturalistic conditions remain unknown (Yamins & Dicarlo, 2016; Brea & Gerstner, 2016).

Here we have examined this issue with multi-electrode recordings in non-human primates performing a naturalistic "foraging" task, in which they learned to recognize a visual image and to associate it with a rewarded location. Learning in this task was abrupt, with most sessions being characterized by large performance improvements over the course of a few trials. This abrupt learning was accompanied by a transient increase in synchronization between neural activity in prefrontal and inferotemporal cortices. Moreover, synchronization increased the most between prefrontal sites that encoded rewards and inferotemporal sites that discriminated between the relevant visual stimuli. In contrast, we did not find local changes in neural firing or oscillatory power that correlated strongly with learning. These results therefore suggest that rapid learning relies on temporal synchronization between cortical sites, rather than local representational changes, a conclusion that was also favored by Hebb (Hebb, 1949).

Results

Abrupt visual learning in a naturalistic behavioral paradigm

In the wild, foraging monkeys rapidly learn to identify locations associated with food (Menzel, 1991). We sought to approximate that behavior under the stationary conditions required for neurophysiology, using "oculomotor foraging" task shown in Figure 1A (Chukoskie, et al., 2013; Krause, et al., 2017). On each trial, animals freely explored a natural scene until their gaze landed within an unmarked *reward zone*. A fixation within the reward zone triggered the release of a few drops of juice and ended the trial.

Within each session, animals were exposed to two different images, each with its own unique reward zone, in a randomly-interleaved fashion. Both the images and the location of the reward zones were initially unfamiliar to the animals. Through repeated presentations of each image, the animals learned to recognize them and to associate them with the corresponding reward zones.

Figure 1B shows the progression of learning within a single example session, considering only one of the two images presented. Each point shows the *response time* (Krause, et al., 2017), defined as the time it took the animal to find the reward zone on each trial. Initially, the typical response time was very high, although the animal occasionally found the reward zone quickly. This poor performance was not due to a lack of engagement, as the animal actively searched the image, making on average 41.5 saccades on each trial (Figure S1A). To maintain engagement during this pre-learning phase, these trials timed out after 20 s, at which point a cue was shown to provide a hint about the correct location (Figure 1A, top).

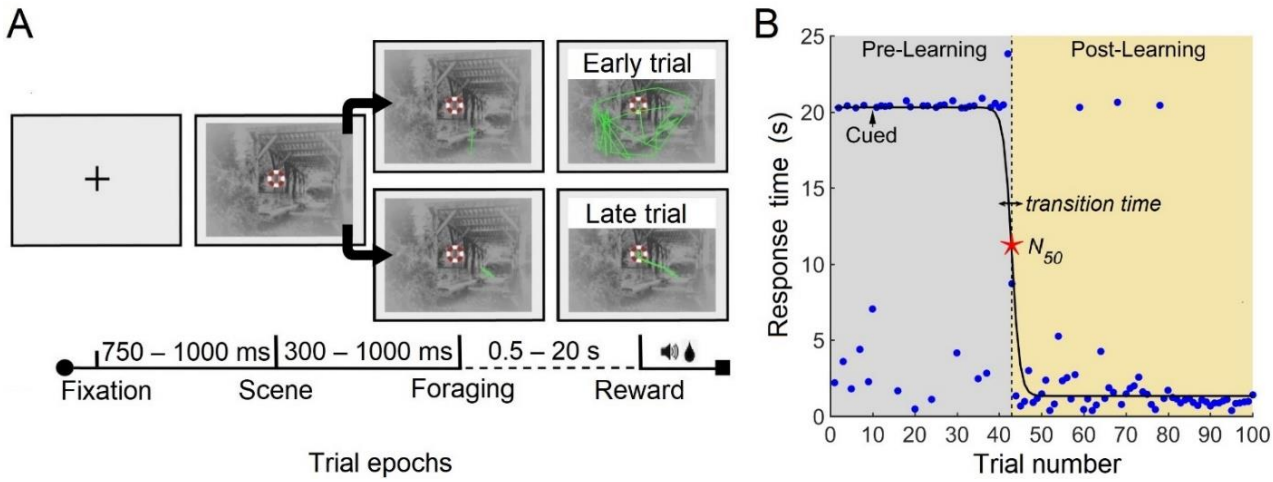

Figure 1. Task diagram and behavior.

(A) An oculomotor "foraging" task was used to study visual learning. Each trial began with the onset of a fixation cross. After fixation was acquired, a natural image appeared, and animals were then free to explore the image in search of a reward zone (marked here with a red-white ring, but not visible to the subject). Fixation on the reward zone led to the release of the reward and the end of the trial. If the reward zone was not found after 15 - 20 s, a cue was given indicating the rewarded location. Each trial was therefore characterized by a Scene epoch, a Foraging epoch, and a Reward epoch. Eye traces (green) are shown for an example early trial (top), when the animal failed to find the reward zone after 20 s, and a late trial (bottom), after learning was complete. Two images were shown in an interleaved manner on every session.

(B) Behavioral performance for an example image. Blue dots indicate the time required to find the target on a single trial, and the black line indicates the fit of a sigmoid function to the data for all trials. The red star indicates the N_{50} trial, estimated from the sigmoid fit as the time required for performance to improve by 50% from its pre-learning to its post-learning state.

On the 43rd trial for this example image, a "moment of insight" occurred, and the typical response time dropped abruptly from 20 s to ~1 s. After the moment of insight, the animal continued to generate saccades at similar rates (3.7 saccades/s before vs. 3.3 saccades/s after; Figure S1B), but the saccades were now generally directed towards the reward zone. Response times remained low on most subsequent trials, suggesting that the animal had successfully learned the association between this image and its reward zone.

To quantify these dynamics, we fit the sequence of response times for each image to a sigmoid function (solid line in Figure 1B). From the sigmoid fits, we extracted three quantities (see Methods). The first was N_{50}, (red star in Figure 1B), defined as the trial at which response time decreased by half from its initial value; we used this value as an objective marker of the trial around which learning was centered. For the example image in Figure 1B, N_{50} occurred on the 43rd trial. A second parameter, the *performance improvement*, was simply the change in response time from the early trials to the later trials for each image. For the example image in Figure 1B, the improvement was 19.0 s. Finally, the *transition time* (arrow in Figure 1B) was defined as the number of trials required for performance to go from 75% to 25% of the maximum response time indicated by the sigmoid fit. For the data shown in Figure 1B, the transition time was 3 trials, which lasted 31.7 seconds in total, indicating that learning was indeed abrupt.

In total, we obtained electrophysiological and behavioral data from sessions involving 50 different images (37 from monkey M and 13 from monkey F). As in the example, the behavioral data were well fit by a sigmoid function (median r^2 = 0.76), with the fit quality not differing significantly between the two animals (one-way ANOVA, $p > 0.05$). From these fits, we calculated that the median performance improvement was 7.71 s (*MAE* 0.41 s); the median transition time was 4.50 trials (median absolute error = 1.78 trials); and the median value of N_{50} was 18. Thus, learning had a pronounced effect on task performance, it happened rapidly, and it usually followed a prolonged period of unsuccessful task performance. These characteristics are typical of abrupt learning (Hebb, 1949; Rubin, et al., 1997).

We also verified that this learning was persistent, by retesting the animals on a subset of the images, many days after the first exposure. On average, response times during the first 10 recall trials for each image decreased by 1.90 s, and the N_{50} value decreased by 12.6 trials (two-way ANOVAs, $p < 0.05$). Thus, our foraging paradigm led to learning that was abrupt but also quite durable, as has been reported for other abrupt learning tasks (Ludmer, et al., 2011).

Cortical dynamics of abrupt learning

To assess the cortical basis of abrupt learning, we recorded simultaneously from 96-channel electrode arrays in the inferotemporal (IT) cortex and the prefrontal cortex (PFC) (Figure 2). Area IT is known to be important for recognizing complex images (Tanaka, 1996; Tsunoda, et al., 2001; Tanaka, et al., 1991), while PFC plays a role in learning arbitrary associations (Asaad, et al., 1998). Lesion studies have suggested that the connections between these two areas are especially important for learning associations between images and spatial locations (Browning, et al., 2005; Hasegawa, et al., 1999; Ranganath, 2006), but the physiological nature of this interaction is unknown (Kornblith & Tsao, 2017). We therefore examined the interactions between sites in IT and PFC, to determine how they evolve with learning.

To focus our analysis, we identified three epochs during each behavioral trial. As shown in Figure 1A, these are the “Scene Onset” epoch, when the image first appeared; the “Foraging” epoch, when search was initiated; and the “Reward” epoch, when the reward was dispensed. These were chosen because retinal stimulation was largely identical within each epoch throughout the progression of learning (see Methods). To characterize learning-related changes in synchronization between PFC and IT, we examined the *oscillatory coherence* between the local field potential (LFP) signals in each area, a commonly used metric that indexes transient changes in corticocortical communication during learning (Antzoulatos & Miller, 2014; Brincat & Miller, 2015; Pesaran, et al., 2021) (see Methods).

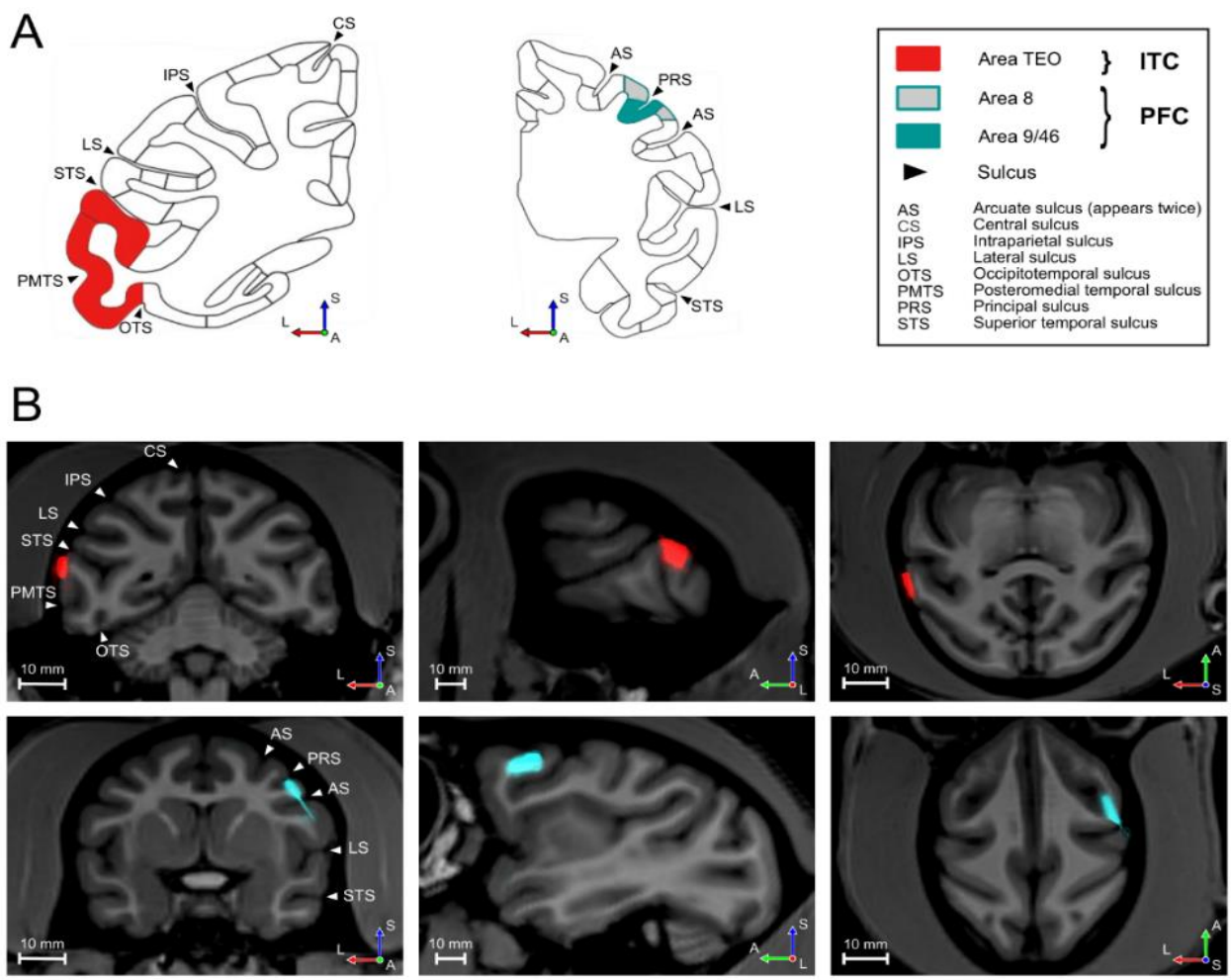

Figure 2. Electrode Array Locations (Monkey F).

Images are shown in neurological convention ("left is left"). L: Left, A: Anterior, S: Superior.
(A) Coronal sections from the Markov et al. (2014) CoreNets atlas showing the brain areas targeted for recording. The sulcal landmarks indicated were used to identify the same regions in each animal's MRI. Due to its curved shape, the arcuate sulcus (AS) appears twice in the coronal PFC sections.
(B) Combined MRI/CT images showing the positions of the IT (top row) and PFC (bottom) arrays in coronal (left), sagittal (center), and axial (right) planes. The preoperative T1-weighted MRI was co-registered with a postoperative CT scan (red, cyan) to verify the array locations. To emphasize the neuroanatomy, the skull and artifacts from other implants have been digitally removed from the CT scan.

To illustrate the general pattern of results, Figure 3A shows the magnitude of synchronization between the two areas, averaged across electrodes and images for both animals. Here, we have grouped trials into a pre-learning phase (before N_{50}, top row), a post-learning phase (after N_{50}, bottom row) and those around the moment of abrupt learning (N_{50}, middle row). The left column, corresponding to the Scene Onset epoch, shows that the appearance of a visual image generally triggered an increase in low-frequency synchronization starting around 200 ms later. This sensory response was consistent throughout the progression of learning (two-way ANOVA, $p>0.05$).

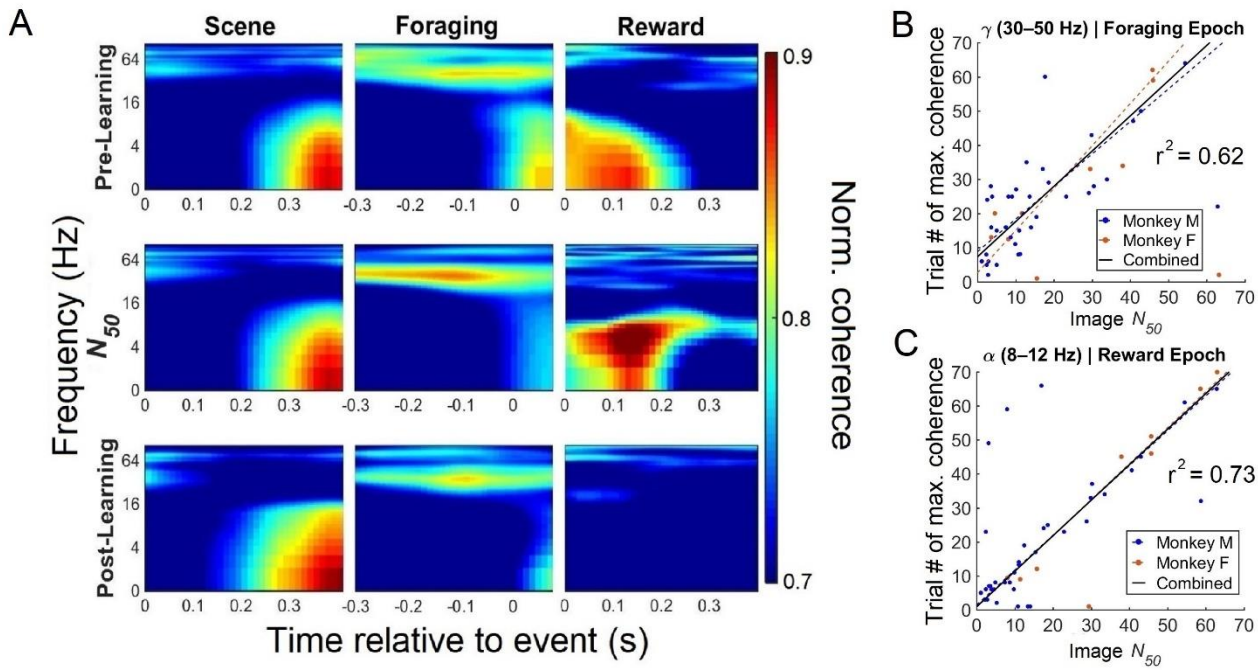

Figure 3. Inferotemporal-prefrontal oscillatory synchronization reflects learning state.

(A) Synchronization of LFP signals between IT and PFC are shown for the three trial epochs (Scene, Foraging, and Reward) at different stages of learning (Pre-Learning, N_{50}, and Post-Learning). Each panel contains a time-frequency plot covering frequencies in the range 1 - 100 Hz and a period of 400 ms around the event that defines each epoch. For the Scene and Reward epochs, t = 0 is the onset of the image and reward respectively. For the Foraging epoch, t = 0 is the onset of the first saccade within a trial. The strength of synchronization is normalized within each frequency and averaged across individual sessions. Around the moment of learning, there was a notable increase in gamma (30-50 Hz) synchronization in the Foraging epoch (middle column, middle row), as well as increased alpha band (8-12 Hz) synchronization during the Reward epoch (Right column, middle row).

(B) Trial number of peak gamma synchronization (30-50 Hz) in the Foraging epoch is plotted against the N_{50} value from the sigmoid fit for the corresponding behavioural data, for each monkey separately (red and blue dots), along with best-fitting regression lines for each animal (red and blue dashed line). The black line indicates the best-fitting regression line for all data combined.

(C) As in (B), but for alpha synchronization during the Reward epoch.

In contrast, the onset of the Foraging epoch (middle column) was accompanied by an increase in gamma band (30–50 Hz) synchronization, which was most prominent around the N_{50} trial, when learning was most evident (middle row). Similarly, the receipt of the reward (right column) was accompanied by a strong increase in alpha-band (8–12 Hz) synchronization that was localized to the trials near N_{50}. These learning-related changes in synchronization did not depend on eye movement behavior, as data were taken from periods of steady fixation, and microsaccade frequency did not change significantly with learning or trial epoch in either animal (two-way ANOVA, $p > 0.05$).

If this synchronization were due to a common input to the two areas, we would expect to find that their oscillations had little or no offset in time (Gregoriou, et al., 2009). This was not the case. For the Foraging epoch, fluctuations in the amplitude of gamma oscillations in IT led those in PFC by an average of 16.1 ms. This timing, along with the concentration of signals in the gamma

band, is consistent with a feedforward direction of information transfer (Adhikari, et al., 2010; Bastos, et al., 2015; Van Kerkoerle, et al., 2014). In contrast, during the Reward epoch, alpha oscillations in PFC led those in IT by an average of 29.5 ms, or roughly a quarter-cycle of alpha. Alpha oscillations are typically associated with feedback signalling, and the relative signal timing we have observed is consistent with this idea (Bastos, et al., 2015; Van Kerkoerle, et al., 2014). We explore these two types of signals in more detail below.

Across sessions, synchronization between IT and PFC accurately predicted changes in behavioral performance. As shown in Figures 3B and 3C, there was a strong correlation between the trials at which synchronization peaked and the behavioral N_{50} trials ($r^2 = 0.62$ for gamma synchronization in the Foraging epoch and $r^2 = 0.73$ for alpha synchronization in the Reward epoch, $p < 0.05$, corrected). These associations were significant for each animal individually (linear regression, trial ~N_{50}, $p < 0.05$, corrected) and when the data were combined across animals (linear regression, trial ~N_{50}, $p < 0.05$, corrected). Moreover, the trials with peak alpha synchronization were correlated with the trials with peak gamma synchronization ($r^2 = 0.72$, $p < 0.01$), indicating that both signals were present in individual sessions (Figure S1C). Thus, the "moment of insight" was associated with an increase in gamma synchronization in the Foraging epoch and an increase in alpha synchronization in the Reward epoch. We therefore focus on these two signals in the following sections.

Selection of sensory signals during abrupt visual learning

To perform the foraging task, the animals had to identify which of the two images was present on each trial, before responding with the appropriate eye movements. Because most IT neurons do not respond to most images (Rolls & Tovee, 1995), visual learning is thought to entail a search for those neurons that are most capable of discriminating between the relevant stimuli (Jacobs, 2009; Dosher & Lu, 2009; Law & Gold, 2009; Bakhtiari, et al., 2020). We therefore examined the extent to which the discriminability of visual images influenced learning.

We first trained a linear decoder to discriminate between the two images presented in each session, using linear discriminant analysis (LDA; see Methods). The decoder was trained based on multi-unit activity in IT, recorded during the Scene Onset epoch. This approach provides a close correlate of perceptual discriminability in other contexts (Majaj, et al., 2015). Consistent with the importance of visual recognition for the task, more difficult image discriminations required more trials to learn: Decoding performance was negatively correlated with the number of trials required to reach N_{50} ($r = -0.59$, $p < 0.01$).

To probe the cortical dynamics of this learning, we used the weights recovered from the LDA to rank each IT electrode according to the selectivity of its multi-unit activity for the two images in each session. These weights provided a measure of informativeness: Sites that were assigned high weights in the LDA were necessary for the population to discriminate between the two images, while those with low weights were not. From this analysis, we extracted the 10 most informative and the 10 least informative IT electrodes in each session.

Figure 4 shows the average strength of interareal synchronization relative to the N_{50} trial, computed in a moving window of five trials (see Methods) and averaged across images; data from only the example image in Figure 1 are shown in Figure S1D. For gamma oscillations in the Foraging epoch (Figure 4A), the synchronization between PFC and IT was initially similar, regardless of the informativeness of the IT electrodes. That is, early in the session,

synchronization strength was similar for the most informative (red) and least informative (blue) IT electrodes. However, for later trials the most informative IT electrodes became significantly more synchronized with PFC (Figure 4B), compared to the least informative IT electrodes (two-way ANOVA, $p < 0.05$, corrected). Interestingly, this synchronization peaked near the N_{50} trial (Figure 4A). After this trial, synchronization between IT and PFC decreased gradually, with the preference for informative IT electrodes also becoming weaker.

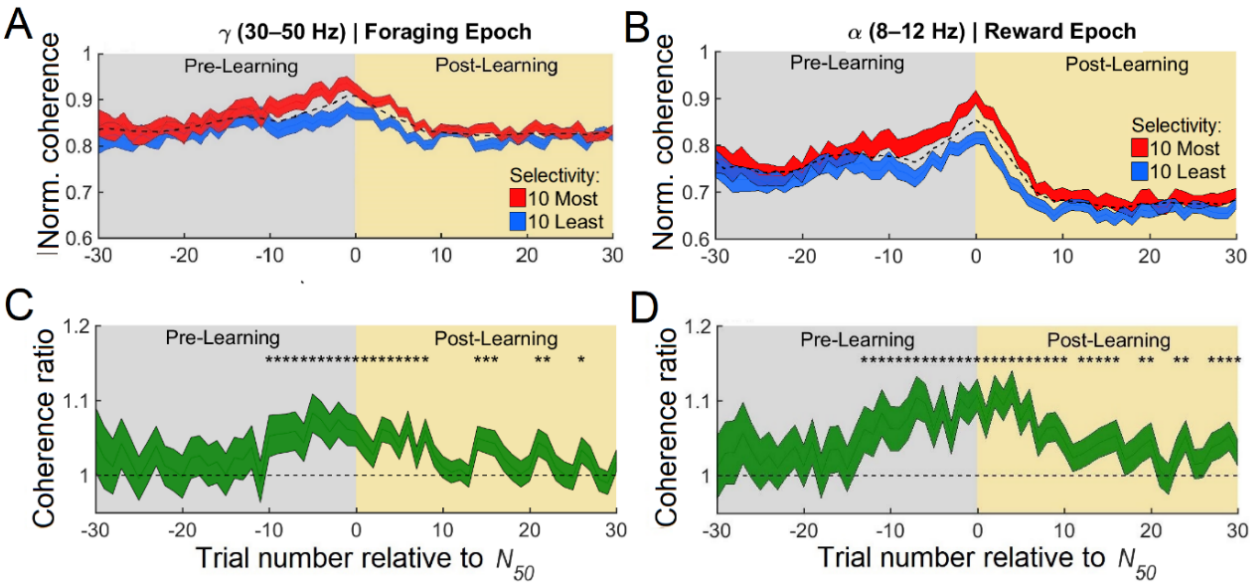

Figure 4. Image selective sites in IT drive synchronization around the time of learning.

(A) Synchronization between IT and PFC is shown for the gamma band (30-50 Hz) in the Foraging epoch. Here data have been averaged across time within an epoch and across images. Results are aligned on the N_{50} trial for each image. The dashed black line represents the grand median of all usable electrode pairs for all sessions. The red and blue lines correspond to the average strength of synchronization between all PFC sites and those IT sites that are most (red) and least (blue) informative about the images shown in each session. The most informative IT electrodes showed higher gamma synchronization (30-50 Hz) with PFC around the moment of learning in the Foraging epoch. Shading around each line indicates standard error (SEM).

(B) As in (A), but for alpha synchronization (8-12 Hz) during the Reward epoch.

(C) The ratio of synchronization strength for the most and least informative electrodes across trials relative to N_{50}. Asterisks indicate trials in which the ratio was significantly different from 1.

(D) As in (C), but for alpha synchronization (8-12 Hz) during the Reward epoch.

A similar pattern was seen for alpha synchronization during the Reward epoch (Figure 4C). Synchronization with PFC was initially similar across IT electrodes, but as trials progressed, the strength of synchronization became stronger for the most informative IT electrodes than for the least informative electrodes (two-way ANOVA, $p < 0.05$, corrected). Here a distinct peak in synchronization is also evident around the N_{50} trial, with a strong preference for informative IT electrodes. This preference also diminished after learning was complete, but it did not disappear entirely, as the increased contribution of informative IT sites to alpha synchronization persisted throughout the post-learning period (two-way ANOVA, $p < 0.05$, corrected). Similar results were obtained when data for each animal were analyzed independently (Figure S3G-H). Thus, both

gamma and alpha synchronization peaked around the N_{50} trial, and long-range synchronization levels were significantly associated with image-selective IT sites.

From Figure 4B and Figure 4D, it is also apparent that the selective contribution of different groups of IT electrodes to interareal synchronization began well before the N_{50} trial. Statistically, the increased gamma synchronization of the most informative IT electrodes compared to the least informative IT electrodes began 10 trials before the N_{50} trial (Figure 4B). For alpha oscillations, the difference emerged 14 trials before the N_{50} trial (Figure 4D). Thus, even considering that our analysis had a resolution of five trials (see Methods), it appears that the selective synchronization of sensory signals began well before the behavioral moment of learning. Overall, our findings suggest a gradual type of neural plasticity that culminates in abrupt learning at the behavioral level.

This kind of selectivity could arise trivially if unresponsive IT electrodes were included in the analysis. Unresponsive electrodes would be neither synchronized with PFC nor selective for images, and so they could exaggerate or even cause the association between synchronization and selectivity shown in Figure 4. To control for this possibility, we recomputed the synchronization analysis shown in Figure 4, after sorting IT electrodes based on the *responsiveness* of their MUA signals (Figure S3A-D), rather than their selectivity. Responsiveness was defined as the change in MUA firing rate in the 400 ms following the release of the reward.

In contrast to the results shown in Figure 4, there was no difference in synchronization between strongly responsive and weakly responsive IT sites (two-way ANOVA, $p > 0.05$), indicating that it is image selectivity, rather than signal quality, that drives synchronization changes during learning. Consistent with this idea, the most (and least) informative electrodes changed from session to session (Figure S2A), which would not occur if defective electrodes were included in the analysis. Moreover, image selectivity by itself did not account for synchronization in other trial epochs or frequency bands (Figure S3E-F).

We conclude that abrupt learning was associated with a gradual increase in synchronization between PFC and the IT sites that carried the most information about the visual stimuli. These changes were specifically related to IT selectivity, as no similar pattern was found when electrodes were sorted according to image selectivity or responsiveness in PFC (Figure S4A-D). Thus, although previous work has found evidence of visual selectivity in PFC (O'Scalaidhe, et al., 1999), this selectivity does not appear to be relevant for abrupt learning in our task.

Contribution of reward signals to abrupt visual learning

Beyond identifying the image on each trial, animals had to learn the association between each image and its corresponding reward zone. Because this association is entirely arbitrary, it must be learned through feedback about the outcome of each trial. We therefore asked whether PFC sites that are sensitive to reward (Sakagami & Pan, 2007) play a role in abrupt learning.

Figure 5 shows the LFP synchronization between PFC and IT, with data again averaged across images relative to the N_{50} trial, as in Figure 4. However, in this case the PFC electrodes have been sorted according to the *responsiveness* of their MUAs to the release of the reward (see Methods). For alpha oscillations during the Reward epoch, the most reward-sensitive (red) PFC sites exhibited greater synchronization with IT than the least reward-sensitive PFC sites (blue) (two-way ANOVA, $p < 0.05$). In contrast to the results shown in Figure 4, this increased synchronization was not aligned on the N_{50} trial, but rather appeared to be a non-specific signal

that persisted across the duration of each session. Furthermore, in contrast to the IT results, the electrodes that provided this reward signal were consistent from image to image (Figure S2B), as would be expected based on the anatomical organization of reward signals in PFC (Sakagami & Pan, 2007). This effect was again not due to poor electrode quality, as there was no similar preferential synchronization for other frequencies and epochs (Figure S4).

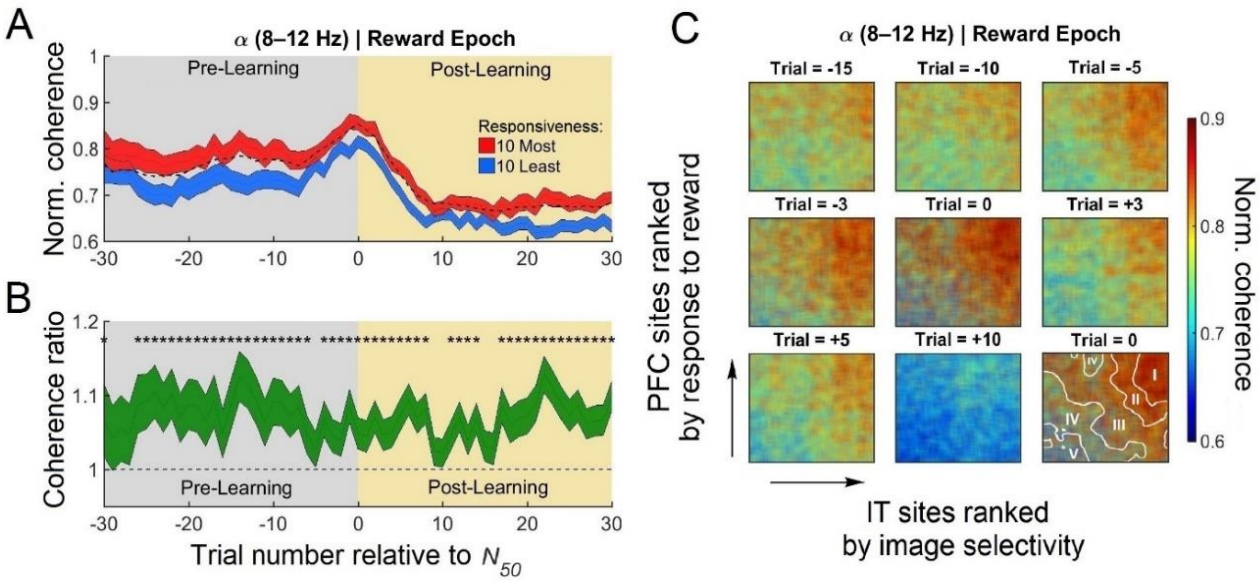

Figure 5. Reward responsive sites in PFC are more synchronized with sites in IT.

(A) Synchronization between IT and PFC is shown for the alpha band (8-12 Hz) in the Reward epoch. As in Figure 4, data have been averaged across time and across sessions, and results are aligned on the N_{50} trial for each image. The dashed black line represents the grand median of all usable electrode pairs for all sessions. The red and blue lines correspond to the average strength of synchronization between all IT sites and those PFC sites that respond most (red) and least (blue) strongly to the receipt of reward. The most reward-responsive PFC electrodes showed higher alpha synchronization with IT, across all trials relative to the onset of learning. Shading around each line indicates standard error (SEM).

(B) The ratio of IT-PFC synchronization strength between reward-responsive and unresponsive PFC electrodes. Asterisks indicate a ratio significantly different from 1.

(C) Alpha synchronization in the Reward epoch, for all IT and PFC electrodes across sessions. Reddish colors indicate strong synchronization, while bluish colors indicate weak synchronization. Different panels correspond to different trials relative to the N_{50} trial. Electrodes in IT were ranked based on much information they carried about images within each session (increasing informativeness from left to right). Electrodes in PFC were ranked based on how strongly they responded following a reward (increasing sensitivity from left to right). Synchronization is generally weak and lacks organization early in each session (top left) but grows stronger around the moment of learning (central panel). Post-learning, synchronization again becomes weaker (bottom middle). Synchronization around N_{50} is clearest between IT electrodes that encode images and PFC electrodes that encode rewards (top right of central panel). The panel on the bottom right highlights this synchronization structure, with five contours drawn at equal distances according to synchronization strength.

The full interaction between reward and sensory signals is shown in Figure 5C, for all sites in both areas. Here each panel corresponds to the data averaged across images for trials relative to the N_{50} trial. As in Figures 4 and 5, the IT electrodes have been ranked according to their informativeness about the images in each session, and this ranking is indicated on the x-axis of each panel. The PFC electrodes have been ranked according to their responsiveness to rewards, and this ranking is indicated on the y-axis of each panel. For the trials near N_{50} (center panel) the strongest alpha synchronization is indeed limited to image-selective sites in IT and reward-sensitive sites in PFC. This is shown by the concentration of reddish colors in the upper right of the panel; the contour plot in the bottom right panel emphasizes that the strongest synchronization occurs between these same subpopulations. For trials long before or after the N_{50} trial, synchronization is generally weaker and distributed more diffusely across sites in both areas.

(Lack of) local correlates of abrupt learning

The results thus far indicate a strong correlate of abrupt learning in the synchronization between IT and PFC. For slower forms of learning, previous work has found changes in selectivity at the single-neuron level in both IT (Kobatake, et al., 1998; Li & DiCarlo, 2010; Logothetis, et al., 1995; De Baene, et al., 2008) and PFC (Freedman, et al., 2001). We therefore looked for similar changes in each area that might reflect abrupt learning.

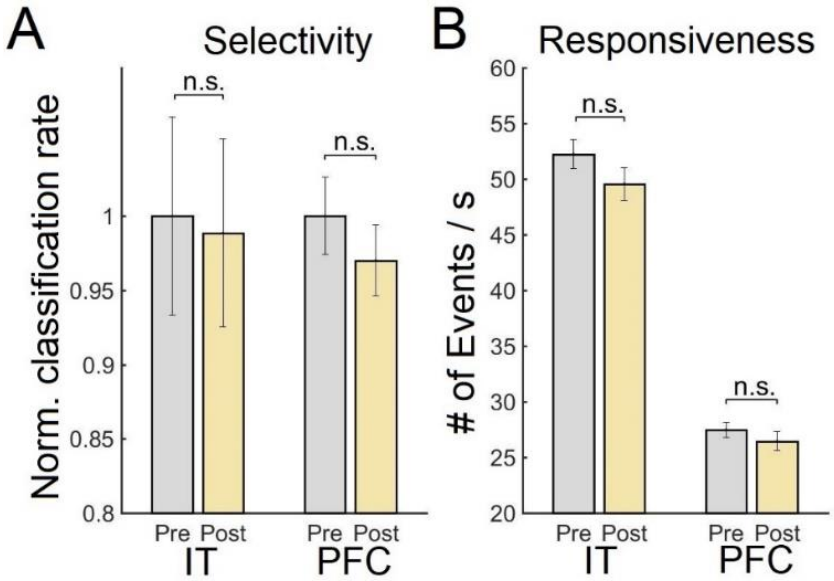

Figure 6. Learning does not affect multi-unit population firing activity or selectivity.

(A) The selectivity of multi-units for scenes was assessed with a linear discriminant analysis (LDA). A window of the first 400 ms of spiking activity after scene onset was used to train the LDA. Neural data were split into pre-learning (silver) and post-learning epochs (gold) for each image, using the sigmoid fits described in Figure 1 and the Methods. Selectivity levels in IT or PFC did not, on average, improve between the pre-learning (gray) and post-learning (yellow) periods. Error bars reflect standard error (SEM) across sessions.

(B) Similarly, learning did not result in changes in responsiveness between the pre- and post-learning sessions.

We used the decoding approach outlined above to assess whether multi-unit population activity showed improved discrimination ability with learning. Decoders were trained on the same images during the Scene Onset epoch for the pre-learning and post-learning stages of each session. The results reveal that decoding performance did not change with learning, in either IT or PFC (Figure 6A). Moreover, we did not find differences in average multi-unit firing rates between the pre- and post-learning periods in either area (Figure 6B) (two-way ANOVA, $p > 0.05$). Thus, it does not appear that neural population activity became more selective for the images during abrupt learning.

Similarly, there was no consistent change in LFP power (Figure S6A-B) or intra-areal synchronization (Figure S6C-D) around the moment of learning. Across trials, there was however a steady decrease in overall PFC power and intra-areal coherence. Similar results have been reported previously, and it has been suggested that they reflect a weaker (Brincat & Miller, 2016) or more selective (Mukai, et al., 2007) engagement with sensory information as learning progresses.

Discussion

Visual learning has traditionally been studied in laboratory tasks that involve extensive training to associate specific stimuli with specific responses. Such training can profoundly alter the underlying cortical circuitry (Chen, et al., 2016; Liu & Pack, 2017; Chowdhury & DeAngelis, 2008) but it does not necessarily reflect the kind of plasticity that occurs in natural settings. We have therefore examined learning in a more naturalistic, free-viewing task that approximates the kind of foraging that primates perform daily in the wild. This behavior is thought to have driven the evolutionary expansion of PFC (Murray, et al., 2020), as well as its connection with IT (Eldridge, et al., 2021). For these reasons, we have studied learning while recording from PFC and IT.

We found that non-human primates engaged in this task abruptly learn to recognize visual images and to associate them with specific reward locations (Figure 1). The strongest neuronal correlates of this learning were found in the synchronization of LFPs between PFC and IT (Figure 3), and this synchronization seems well-suited to link informative visual inputs with signals about rewarded outcomes (Figures 4, 5). The strength of this synchronization was greatest around the moment of insight (Figures 4, 5), but the tendency for informative IT signals to be more synchronized with PFC persisted well beyond the N_{50} trial (Figure 4). Local correlates of learning were largely absent in both IT and PFC (Figure 6). These results therefore identify a cortical circuit capable of supporting abrupt visual plasticity.

Theories of abrupt learning

Hebb (1949) was among the first to evince a theory of abrupt learning, hypothesizing that the underlying neurophysiological mechanisms share some properties with those that support learning on longer timescales. More recent work has provided some support for this idea, by showing that rapid learning exhibits stimulus specificity similar to that observed with slower learning (Rubin et al., 1997, 2002).

Computational work has explained both types of learning based on a process that selects the most informative sensory neurons for a given task (Jacobs, 2009; Bakhtiari, et al., 2020; Lin, et al., 2017). This proposition is entirely consistent with the current results (Figure 4), as well as

previous findings in other brain regions (Law & Gold, 2010; Liu & Pack, 2017). Moreover, in accordance with psychophysical results, we find that the selection of informative sensory inputs relies on explicit feedback (Rubin, et al., 2002) in the form of rewards.

For slower forms of learning, there has been some question about whether reward signals reaching sensory cortex are stimulus-specific (FitzGerald, et al., 2013). Our data show that the synchronization for reward-related signals is non-specific with respect to learning, being roughly constant throughout the duration of each session (Figure 5). However, the moment of insight is accompanied by a marked increase in sensory specificity: The greatest synchronization occurs for image-selective sites in IT (Figure 5C). One explanation is therefore that, during learning, non-specific feedback about rewards is amplified according to the informativeness of the sensory sites for the perceptual task (Stanisor, et al., 2013).

The mechanism by which reward signals are connected to informative sensory signals is likely related to that of top-down attention, which is important for most kinds of learning (Byers & Serences, 2012; Watanabe & Sasaki, 2015). The interplay of these different kinds of feedback is captured effectively by models that typically operate on longer timescales (Roelfsema & van Ooyen, 2005; Roelfsema, et al., 2010). In these models, a successful trial (i.e., one followed by reward) is followed by an attentional signal that selectively targets the upstream neurons that led to the rewarded outcome.

Our data (Figure 3) are consistent with this idea if we consider gamma synchronization to be a correlate of covert attention. Previous work (Gregoriou, et al., 2009) has indeed shown that such synchronization between prefrontal and visual cortices occurs during visual attention, with time lags resembling those found in our data. Although we have not controlled attention directly in our experiments, a speculative interpretation of our data is that learning occurs when attention is directed to the most informative visual features in each image. This would account for the segregation of IT sites based on informativeness that occurs around the moment of learning (Figure 4). The most informative signals in IT would then propagate up the hierarchy to PFC, which is consistent with the relative timing of signals we observed, as well as much previous work (Van Kerkoerle, et al., 2014; Bosman, et al., 2012).

Role of oscillations in abrupt learning

Hebb's favored mechanism for learning took the form of cell assemblies that become connected after being repeatedly activated at the same time. Modern investigations of this hypothesis in humans have confirmed that long-range synchronization between different brain regions is a reliable correlate of certain kinds of learning (Miltner, et al., 1999; Verbeke, et al., 2021). This coherence has often been found in the gamma band (Miltner, et al., 1999; Jutras, et al., 2009; Popescu, et al., 2009; Igarashi, et al., 2014), which is also associated with learning in our task (Figures 3, 6). Although the relationship between gamma oscillations and learning was correlational in this work, there is some evidence for a causal connection as well (Krause, et al., 2017; Santernecchi, et al., 2019; Cho, et al., 2020).

In rodents, gamma oscillations are often nested within theta oscillations, and this coupling has been shown to be important for associative learning (Tort, et al., 2009). Moreover, the theta rhythm itself is well-known for its role in learning, particularly in the hippocampus (Benchenane, et al., 2010; DeCoteau, et al., 2007; Jutras, et al., 2013), but theta did not seem to correlate with abrupt learning in our data (Figure 3). Rather, the clearest correlate was found for

PFC-driven oscillations in the alpha band (Figure 4), which are also implicated in human studies of insight (Sprugnoli, et al., 2017; Santernecchi, et al., 2019).

We found that alpha synchronization seemed most related to the release of rewards within each trial (Figure 5). This makes sense in light of previous findings, in which alpha oscillations in PFC are modulated by dopaminergic signals arriving via the striatum (Puig & Miller, 2012). From PFC, our data suggest that these signals flow in a feedback direction to visual cortex, given their appearance in the alpha band (Bastos, et al., 2015; Van Kerkoerle, et al., 2014) and their timing relative to IT.

Abrupt learning in the prefrontal cortex

Most previous work has suggested that PFC plays a role in facilitating learning but that it is not itself the primary site of long-lasting plasticity (Cohen, et al., 2004; Miller & Cohen, 2001; Petrov, et al., 2005; Ott & Nieder, 2019; Meyers, et al., 2012; Shadmehr & Holcomb, 1997; Passingham, et al., 2000; Sakagami & Pan, 2007). Instead, it might be involved in discerning the rules that map stimuli to responses for a given task (Durstewitz, et al., 2010). The encoding of these rules can appear abruptly in PFC for novel associations (Cromer, et al., 2011) or for reversals of previously learned associations (Pasupathy & Miller, 2005). However, learned improvements in stimulus encoding are less common, and there is even evidence that stimulus encoding decreases with learning (Brincat & Miller, 2016), suggesting that PFC likely does not learn novel stimuli on short timescales. Our results (Figures 3, 4) are consistent with this idea, since there is little evidence of enduring changes in image selectivity in the PFC neurons we recorded (Figure 6).

For visuomotor associations, the connection between PFC and IT is known to be critical (Browning, et al., 2005; Bussey, et al., 2002). Lesions that disconnect these areas severely impair visuomotor learning (Gutnikov, et al., 1997) and especially "object in place" learning, a kind of rapid learning that resembles our foraging paradigm (Browning, et al., 2005; Browning & Gaffan, 2008). A more mechanistic role for PFC is suggested by the finding that neurons in this area help to solve the "credit assignment" problem. This refers to the challenge faced by the brain in identifying synaptic connections that can be strengthened to improve performance on a given task. Asaad et al. (2017) reported that selective visual signals were found in populations of PFC neurons that also represented reward outcomes, as would be necessary to solve the credit assignment problem. Our results suggest that this information emerges dynamically through communication between subpopulations of IT neurons that encode the relevant stimuli and PFC neurons that encode the reward (Figure 5C).

Abrupt learning in the visual cortex

While previous work has found rapid learning in individual IT neurons (Tovee, et al., 1996; Li & DiCarlo, 2010), we did not find evidence for this at the population level (Figure 6). One possibility is that learning affected different classes of neurons differently (Khan, et al., 2018), which would not have been reflected in our population-level results, as we do not have a reliable way of assessing molecularly-defined cell types in our sample.

With extended training, changes in neural selectivity have been observed in IT (Logothetis, et al., 1995; Adab, et al., 2014), V4 (Yang & Maunsell, 2004; Adab & Vogels, 2011), V2 (Ghose & Maunsell, 2002), and V1 (Schoups, et al., 2001; Li, et al., 2004) These results are

generally consistent with the observation that the adult visual system changes quite slowly with training (Watanabe & Sasaki, 2015). Far less is known about the effects of rapid learning in the visual cortex, but Wang and Dragoi (2015) reported a transient, learning-related increase in spike-field coherence in area V4. This coherence increase was found in the theta band and within a single area but followed a similar time-course to the changes in long-range synchronization we report here (Figure 3).

Other brain structures involved in abrupt learning

The most dramatic form of abrupt learning is one-shot learning, in which only a single instance of a stimulus is provided (Cook & Fagot, 2009). This kind of learning is closely related to episodic memory, which depends critically on the hippocampus (Eichenbaum, 2000). Interactions between PFC and hippocampus have been shown to correlate with learning on short timescales in monkeys (Brincat & Miller, 2015) and rodents (Benchenane, et al., 2010). In humans, the hippocampus is recruited by PFC when one-shot learning is dictated by the demands of a task (Lee, et al., 2015). Thus, it might be that PFC establishes the conditions for learning, but that information is initially stored in the hippocampus (McClelland, et al., 1995) and then later consolidated into long-term memory (Tse, et al., 2007).

For tasks that involve a saccadic response, neurons in the caudate nucleus facilitate saccades toward rewarded locations, and these signals can update rapidly as contingencies change (Kawagoe, et al., 1998; Pasupathy & Miller, 2005; Watanabe & Hikosaka, 2005). Indeed, Williams & Eskandar (2006) found that firing rates in the caudate correlate with the rate of learning in a task that requires learning to saccade to a particular visual stimulus. The output of these neurons could therefore be linked to the synchronization changes we have observed (Figure 4), which also correlate with the rate of learning.

This connection between dopaminergic cells and learning in PFC has been studied by Puig and Miller (2012), who showed that dopaminergic drugs in PFC can modulate associative learning. Specifically, antagonists of some dopamine receptors block the formation of new associations, but they do not impair the recall of those already established. Putting these results together, it could be that dopamine released from the caudate facilitates the formation of new or stronger connections between informative sites in IT and longer-term storage in hippocampus, with the PFC playing a permissive role in “switching on” rapid learning (Cohen, et al., 2004; Miller & Cohen, 2001; Petrov, et al., 2005; Ott & Nieder, 2019). Previous work has also highlighted a role for the amygdala in this process (Paton, et al., 2006; Ludmer, et al., 2011).

Alternative interpretations

In addition to providing signals about reward outcomes, the PFC plays a role in arousal, working memory, and attention (Sakagami & Pan, 2007), all of which are important for learning (Watanabe & Sasaki, 2015). Though it is notoriously difficult to disentangle these factors (Maunsell, 2004), we have shown evidence that none of them alone is sufficient to explain our findings. First, non-specific effects like arousal would not account for the preference for informative IT electrodes in the synchronization between IT and PFC (Figure 4). Thus, while we favor the interpretation of a non-specific signal emanating from PFC (Figure 5), we suggest that it is more parsimonious to think of it as carrying information about rewards, rather than arousal

per se (Roelfsema & van Ooyen, 2005). Second, working memory might account for the retention of visual associations within each testing session, and it has been often associated with both gamma (Salazar, et al., 2012) and alpha synchronization (Palva & Palva, 2011; Neupane, et al., 2017). However, by itself it cannot account for the animals' ability to remember the associations many days later.

This long-term recall also supports the idea that changes in behavioral performance in our foraging task reflect genuine visual learning. This is in contrast to an alternative possibility, namely that the data reflect a shift in behavioral strategy between early and later trials. Such shifts might be expected to alter the dynamics of prefrontal activity (Ebitz, et al., 2018), but it is not clear why they would lead to the pattern of synchronization changes we have observed (Figure 3), why this pattern would emphasize informative IT electrodes (Figure 4), or why it would have effects that persisted many weeks later.

Finally, we have not specifically controlled top-down attention in this task, as part of our goal was to simulate learning under natural conditions. Attention could therefore have played various roles in learning or overall task performance (Serences & Kastner, 2014). Of these roles, the most commonly observed consequence of attention is an improvement in sensory coding, which we did not observe in our data (Figure 6). However, our data are consistent with a different role for attention, namely that of selecting relevant visual inputs based on rewards (Baruni, et al., 2015; Serences & Kastner, 2014). As mentioned above, such a role is consistent with both the gamma synchronization we observe (Gregoriou, et al., 2009) and its specificity for informative sensory signals (Figure 4). Previous work has found that this kind of attentional mechanism is especially important for extracting relevant information from complex stimuli (Pestilli, et al., 2011; Niv, et al., 2015) of the kind we have used in our foraging task, and so it could have been a factor in our data as well.

Conclusion

We have shown that visual learning happens abruptly when animals use eye movements to forage for a rewarded location in an image. In contrast to most previous studies of visual learning, our paradigm made use of natural images and unconstrained eye movement behaviors. As a result, our results might provide greater insight into the kind of learning that occurs outside of a laboratory. Moreover, our paradigm facilitates observation of neural signals throughout the entire trajectory of learning.

In our electrophysiological data, abrupt learning was accompanied by increased synchronization between reward signals in PFC and image-selective signals in IT. Time-frequency analysis suggests that this synchronization has two components: a feedforward component that is active during inspection of the image and a feedback component that is active upon receipt of a reward. This pattern of activity is compatible with predictions of computational models that assign specific functions to feedforward and feedback pathways during visual learning (Roelfsema, et al., 2010; Ahissar & Hochstein, 2004). Both signals become more attuned to informative sensory signals at the "moment of insight", highlighting the role for distributed neural circuits in facilitating the rapid acquisition of new sensory knowledge.

STAR★Methods

Detailed methods are provided in the online version of this paper and include the following:

- KEY RESOURCES TABLE
- RESOURCE AVAILABILITY
  - Lead contact
  - Materials availability
  - Data and code availability
- EXPERIMENTAL SETUP
  - Animal preparation
  - Behavioral tasks
  - Eye calibration
- BEHAVIORAL DATA ANALYSIS
  - Response modeling
  - Saccadic eye movements
- ELECTROPHYSIOLOGICAL DATA ANALYSIS
  - Processing of raw data
  - Trial epoch selection
  - Calculation of spectral power
  - Synchronization
  - Calculation of cross-correlation and lags
  - Multi-unit analysis
  - Statistics

Supplemental Information

Supplemental information can be found online at TBD.

Acknowledgements

This work was funded by a grant from the CIHR to C.C.P. (MOP-115178) and a graduate student fellowship to B.A.C. from NSERC. We thank Dr. Shahab Bakhtiari and Tugce Gurbuz for helpful comments and discussions.

Author Contributions

M.R.K. and C.C.P. designed the study. M.R.K. and T.P.Z. performed the experiments. B.A.C. analyzed the data. B.A.C., M.R.K. and C.C.P. wrote the paper.

Declaration of Interests

The authors declare no competing interests.

References

Adab, H. Z., Popivanov, I. D., Vanduffel, W. & Vogels, R., 2014. Perceptual learning of simple stimuli modifies stimulus representations in posterior inferior temporal cortex. *J. Cogn. Neurosci.,* 26(10), pp. 2187-2200.

Adab, H. Z. & Vogels, R., 2011. Practicing coarse orientation discrimination improves orientation signals in Macaque cortical area V4. *Curr. Biol.,* 21(19), pp. 1661-1666.

Adhikari, A., Sigurdsson, T., Topiwala, M. A. & Gordon, J. A., 2010. Cross-correlation of instantaneous amplitudes of field potential oscillations: A straightforward method to estimate the directionality and lag between brain areas. *J. Neurosci. Methods,* 191(2), pp. 191-200.

Ahissar, M. & Hochstein, S., 1997. Task difficulty and the specificity of perceptual learning. *Nature,* 387(6631), pp. 401-406.

Ahissar, M. & Hochstein, S., 2004. The reverse hierarchy theory of visual perceptual learning. *Trends Cogn. Sci. ,* 8(10), pp. 457-464.

Antzoulatos, E. G. & Miller, E. K., 2014. Increases in functional connectivity between prefrontal cortex and striatum during category learning. *Neuron,* 83(1), pp. 216-225.

Asaad, W. F., Lauro, P. M., Perge, J. A. & Eskander, E. N., 2017. Prefrontal neurons encode a solution to the credit-assignment problem. *J. Neurosci.,* 37(29), pp. 6995-7007.

Asaad, W. F., Rainer, G. & Miller, E. K., 1998. Neural activity in the primate prefrontal cortex during associative learning. *Neuron,* 21(6), pp. 1399-1407.

Babadi, B. & Brown, E. N., 2004. A review of multitaper spectral analysis. *IEEE. Trans. Biomed. Eng.,* 61(5), pp. 1555-1564.

Bakhtiari, S., Awada, A. & Pack, C. C., 2020. Influence of stimulus complexity on the specificity of visual perceptual learning. *J. Vis.,* 20(13), pp. 1-19.

Baruni, J. K., Lau, B. & Salzman, D. C., 2015. Reward expectation differentially modulates attentional behavior and activity in visual area V4. *Nat. Neurosci.,* Volume 18, pp. 1656-1663.

Bastos, A. M. et al., 2015. Visual areas exert feedforward and feedback influences through distinct frequency channels. *Neuron,* 85(2), pp. 390-401.

Benchenane, K. et al., 2010. Coherent theta oscillations and reorganization of spike timing in the hippocampal-prefrontal network upon learning. *Neuron,* 66(6), pp. 921-936.

Benjamini, Y. & Yekutieli, D., 2005. False discovery rate - adjusteed multiple confidence intervals for selected parameters. *J. Am. Stat. Assoc.,* 100(469), pp. 71-81.

Bichot, N. P., Schall, J. D. & Thompson, K. G., 1996. Visual feature selectivity in frontal eye fields induced by experience in mature macaques. *Nature,* Volume 381, pp. 697-699.

Bosman, C. A. et al., 2012. Attentional stimulus selection through selective synchronization between monkey visual areas. *Neuron,* 75(5), pp. 875-888.

Brady, T. F., Konkle, T., Alvarez, G. A. & Oliva, A., 2008. Visual long-term memory has a massive storage capacity for object details. *Proc. Natl. Acad. Sci. USA,* 105(38), pp. 14325-14329.

Brea, J. & Gerstner, W., 2016. Does computational neuroscience need new synaptic learning paradigms?. *Curr. Opin. Behav. Sci.,* Volume 11, pp. 61-66.

Brincat, S. L. & Miller, E. K., 2015. Frequency-specific hippocampal-prefrontal interactions during associative learning. *Nat. Neurosci.,* Volume 18, pp. 576-581.

Brincat, S. L. & Miller, E. K., 2016. Prefrontal cortex networks shift from external to internal modes during learning. *J. Neurosci.,* Volume 36, pp. 9739-9754.

Browning, P. G., Easton, A., Buckley, M. J. & Gaffan, D., 2005. The role of prefrontal cortex in object-in-place learning in monkeys. *Eur. J. Neurosci.,* 22(12), pp. 3281-3291.

Browning, P. G. & Gaffan, D., 2008. Prefrontal cortex function in the representation of temporally complex events. *J. Neurosci.,* 28(15), pp. 3934-3940.

Bussey, T. J., Wise, S. P. & Murray, E. A., 2002. Interaction of ventral and orbital prefrontal cortex with inferotemporal cortex in conditional visuomotor learning. *Behav. Neurosci.,* 116(4), pp. 703-715.

Byers, A. & Serences, J. T., 2012. Exploring the relationship between perceptual learning and top-down attentional control. *Vision Res.,* Volume 74, pp. 30-39.

Chen, Y., Matheson, L. E. & Sakata, J. T., 2016. Mechanisms underlying the social enhancement of vocal learning in songbirds. *Proc. Natl. Acad. Sci. USA,* 113(24), pp. 6641-6646.

Cho, K. K. et al., 2020. Cross-hemispheric gamma synchrony between prefrontal parvalbumin interneurons supports behavioral adaptation during rule shift learning. *Nat. Neurosci.,* Volume 23, pp. 892-902.

Chowdhury, S. A. & DeAngelis, G. C., 2008. Fine discrimination training alters the causal contribution of macaque area MT to depth perception. *Neuron,* 60(2), pp. 367-377.

Chukoskie, L. et al., 2013. Learning where to look for a hidden target. *Proc. Natl. Acad. Sci. USA,* 110(Suppl 2), pp. 10438-10445.

Cohen, J. D., Aston-Jones, G. & Gilzenrat, M. S., 2004. A systems-level perspective on attention and cognitive control: guided activation, adaptive gating, conflict monitoring, and exploitation versus exploration. In: M. I. Posner, ed. *Cognitive Neuroscience of Attention.* 2nd ed. New York: The Guilford Press, pp. 71-90.

Cook, R. & Fagot, J., 2009. First trial rewards promote 1-trial learning and prolonged memory in pigeon and baboon. *Proc. Natl. Acad. Sci. USA,* 106(23), pp. 9530-9533.

Corain, L. & Salmaso, L., 2007. A critical review and a comparative study on conditional permutation tests for two-way ANOVA. *Commun. Stat. Simul. Comput.,* 36(4), pp. 791-805.

Cornelissen, F. W., Peters, E. M. & Palmer, J., 2012. The eyelink toolbox: eye tracking with MATLAB and the Psychophysics Toolbox. *Behav. Res. Methods, Instruments, & Computers,* Volume 34, pp. 613-617.

Cromer, J. A., Machon, M. & Miller, E. K., 2011. Rapid association learning in the primate prefrontal cortex in the absence of behavioral reversals. *J. Cogn. Neurosci.,* 23(7), pp. 1823-1828.

De Baene, W., Ons, B., Wagemans, J. & Vogels, R., 2008. Effects of category learning on the stimulus selectivity of macaque inferior temporal neurons. *Learn. Mem.,* Volume 15, pp. 717-727.

DeCoteau, W. E. et al., 2007. Learning-related coordination of striatal and hippocampal theta rhythms during acquisition of a procedural maze task. *Proc. Natl. Acad. Sci. USA,* 104(13), pp. 5644-5649.

Dosher, B. A. & Lu, Z.-L., 2009. Hebbian reweighting on stable representations in perceptual learning. *Learn. Percept.,* 1(1), pp. 37-58.

Durstewitz, D., Vittoz, N. M., Floresco, S. B. & Seamans, J. K., 2010. Abrupt transitions between prefrontal neural ensemble states accompany behavioral transitions during rule learning. *Neuron,* 66(3), pp. 438-448.

Ebitz, B. R., Albarran, E. & Moore, T., 2018. Exploration disrupts choice-predictive signals and alters dynamics in prefrontal cortex. *Neuron,* 97(2), pp. 450-461.e9.

Eichenbaum, H., 2000. A cortical-hippocampal system for declarative memory. *Nat. Rev. Neurosci.,* 1(1), pp. 41-50.

Eldridge, M. A., Hines, B. E. & Murray, E. A., 2021. The visual prefrontal cortex and anthropoids: interaction with temporal cortex in decision making and its role in the making of 'visual animals'. *Curr. Opin. Behav. Sci.,* Volume 41, pp. 22-29.

Fedorov, A. et al., 2012. 3D Slicer as an image computing platform for the Quantitative Imaging Network. *Magn. Reson. Imaging,* 30(9), pp. 1323-1341.

FitzGerald, T. H., Friston, K. J. & Dolan, R. J., 2013. Characterising reward outcome signals in sensory cortex. *NeuroImage,* Volume 83, pp. 329-334.

Freedman, D. J., Riesenhuber, M., Poggio, T. & Miller, E. K., 2001. Categorical representation of visual stimuli in the primate prefrontal cortex. *Science,* Volume 291, pp. 312-316.

Gallistel, C. R., Fairhurst, S. & Balsam, P., 2004. The learning curve: Implications of a quantitative analysis. *Proc. Natl. Acad. Sci. USA,* 101(36), pp. 13124-13131.

Ghose, G. M. & Maunsell, J. H., 2002. Attentional modulation in visual cortex depends on task timing. *Nature,* Volume 419, pp. 616-620.

Gregoriou, G. G., Gotts, S. J., Zhou, H. & Desimone, R., 2009. High-frequency, long-range coupling between prefrontal and visual cortex during attention. *Science,* 324(5931), pp. 1207-1210.

Gutnikov, S. A., Ma, Y.-Y. & Gaffan, D., 1997. Temporo-frontal disconnection impairs visual-visual paired association learning but not configural learning in Macaca monkeys. *Eur. J. Neurosci.,* 9(7), pp. 1524-1529.

Harris, A. Z. & Gordon, J. A., 2015. Long-range neural synchrony in behavior. *Annu. Rev. Neurosci.,* Volume 38, pp. 171-194.

Hasegawa, I., Hayashi, T. & Miyashita, Y., 1999. Memory retrieval under the control of the prefrontal cortex. *Ann. Med.,* Volume 31, pp. 380-387.

Havlicek, L. L. & Peterson, N. L., 1976. Robustness of the Pearson correlation against violations of assumptions. *Percept. Mot. Skills,* 43(3), pp. 1319-1334.

Hebb, D. O., 1949. *The organization of behavior: a neuropsychological theory.* New York: Wiley.

Horwitz, G. D., Batista, A. P. & Newsome, W. T., 2004. Direction-selective visual responses in macaque superior colliculus induced by behavioral training. *Neurosci. Lett.,* 366(3), pp. 315-319.

Igarashi, K. M. et al., 2014. Coordination of entorhinal–hippocampal ensemble activity during associative learning. *Nature,* Volume 510, pp. 143-147.

Jacobs, R. A., 2009. Adaptive precision pooling of model neuron activities predicts the efficiency of human visual learning. *J. Vis.,* 9(4)(22), pp. 1-15.

Jutras, M. J., Fries, P. & Buffalo, E. A., 2009. Gamma-band synchronization in the macaque hippocampus and memory formation. *J. Neurosci.,* Volume 29, pp. 12521-12531.

Jutras, M. J., Fries, P. & Buffalo, E. A., 2013. Oscillatory activity in the monkey hippocampus during visual exploration and memory formation. *Proc. Natl. Acad. Sci. USA,* 110(32), pp. 13144-13149.

Kar, K. & DiCarlo, J. J., 2021. Fast recurrent processing via ventrolateral prefrontal cortex is needed by the priamte ventral stream for robus core visual object recognition. *Neuron,* 109(1), pp. 164-176.e5.

Kawagoe, R., Takikawa, Y. & Hikosaka, O., 1998. Expectation of reward modualtes cognitive signals in the basal ganglia. *Nat. Neurosci.,* Volume 1, pp. 411-416.

Khan, A. G. et al., 2018. Distinct learning-induced changes in stimulus selectivity and interactions of GABAergic interneuron classes in visual cortex. *Nat. Neurosci.,* Volume 21, pp. 851-859.

Kobatake, E., Wang, G. & Tanaka, K., 1998. Effects of shape-discrimination training on the selectivity of inferotemporal cells in adult monkeys. *J. Neurophysiol.,* 80(1), pp. 324-330.

Kornblith, S. & Tsao, D. Y., 2017. How thoughts arise from sights: inferotemporal and prefrontal contributions to vision. *Curr. Opin. Neurobiol.,* Volume 46, pp. 208-218.

Krause, M. R. et al., 2017. Transcranial Direct Current Stimulation Facilitates Associative Learning and Alters Functional Connectivity in the Primate Brain. *Curr. Biol.,* 27(20), pp. 3086-3096.

Kravitz, D. J. et al., 2013. The ventral visual pathway: an expanded neural framework for the processing of object quality. *Trends Cogn. Sci.,* 17(1), pp. 26-49.

Laamerad, P., Guitton, D. & Pack, C. C., 2020. Eye movements shape visual learning. *Proc. Natl. Acad. Sci. USA,* 117(14), pp. 8203-8211.

Law, C.-T. & Gold, J. I., 2009. Reinforcement learning can account for associative and perceptual learning on a visual-decision task. *Nat. Neurosci.,* Volume 12, pp. 655-663.

Law, C.-T. & Gold, J. I., 2010. Shared Mechanisms of Perceptual Learning and Decision Making. *Top. Cogn. Sci.,* 2(2), pp. 226-238.

Lee, S. W., O'Doherty, J. P. & Shimojo, S., 2015. Neural computations mediating one-shot learning in the human brain. *PLoS Biol.,* 13(4), p. e1002137.

Li, N. & DiCarlo, J. J., 2010. Unsupervised natural visual experience rapidly reshapes size-invariant object representation in inferior temporal cortex. *Neuron,* 67(6), pp. 1062-1075.

Lin, Z., Dosher, B. A. & Lu, Z.-L., 2017. Mixture of easy trials enables transient and sustained perceptual improvements through priming and perceptual learning. *Sci. Rep.,* 7(7421), pp. 1-9.

Liu, L. D. & Pack, C. C., 2017. The contribution of area MT to visual motion perception depends on training. *Neuron,* Volume 95, pp. 436-446.

Li, W., Piëch, V. & Gilbert, C. D., 2004. Perceptual learning and top-down influences in primary visual cortex. *Nat. Neurosci.,* Volume 7, pp. 651-657.

Ljungberg, T., Apicella, P. & Schultz, W., 1992. Responses of monkey dopamine neurons during learning of behavioral reactions. *J. Neurophysiol.,* 67(1), pp. 145-163.

Logothetis, N., Pauls, J. & Poggio, T., 1995. *Spatial Reference Frames for Object Recognition. Tuning for Rotations in Depth.,* Cambridge, MA, USA: MIT Artificial Intelligence Laboratory, MIT School of Science: Center for Biological & Computational Learning..

Ludmer, R., Dudai, Y. & Rubin, N., 2011. Uncovering camouflage: amygdala activation predicts long-term memory of induced perceptual learning. *Neuron,* 69(5), pp. 1002-1014.

Majaj, N. J., Hong, H. & Solomon, E. A., 2015. Simple learned weighted sums of inferior temporal neuronal firing rates accurately predict human core object recognition performance. *J. Neurosci.,* 35(39), pp. 13402-13418.

Markov, N. T. et al., 2014. A weighted and directed interareal connectivity matrix for macaque cerebral cortex. *Cereb. Cortex,* 24(1), pp. 17-36.

Maunsell, J. H., 2004. Neuronal representations of cognitive state: reward or attention?. *Trends Cogn. Sci.,* 8(6), pp. 261-265.

McClelland, J. L., McNaughton, B. L. & O'Reilly, R. C., 1995. Why there are complementary learning systems in the hippocampus and neocortex: Insights from the successes and failures of connectionist models of learning and memory. *Psychol. Rev.,* 102(3), pp. 419-457.

Menzel, C. R., 1991. Cognitive aspects of foraging in Japanese monkeys. *Anim. Behav.,* 41(3), pp. 397-402.

Meyers, E. M., Qi, X.-L. & Constantinidis, C., 2012. Incorporation of new information into prefrontal cortical activity after learning working memory tasks. *Proc. Natl. Acad. Sci. USA,* 109(12), pp. 4651-4656.

Miller, E. K. & Cohen, J. D., 2001. An integrative theory of prefrontal cortex function. *Annu. Rev. Neurosci.,* Volume 24, pp. 167-202.

Miltner, W. H. R. et al., 1999. Coherene of gamma-band EEG activity as a basis for associative learning. *Nature,* Volume 397, pp. 434-436.

Mitchell, D. B., 2006. Nonconscious priming after 17 years: invulnerable implicit memory. *Psychol. Sci.,* 17(11), pp. 925-929.

Mitra, P. & Bokil, H., 2008. *Observed Brain Dynamics.* s.l.:Oxford University Press.

Mukai, I. et al., 2007. Activations in visual and attention-related areas predict and correlate with the degree of perceptual learning. *J. Neurosci.,* 27(42), pp. 11401-11411.

Murray, E., Wise, S. P., Baldwin, M. K. & Graham, K. S., 2020. *The Evolutionary Road to Human Memory.* 1st ed. Great Claredon Street, Oxford, United Kingdom: Oxford University Press.

Neupane, S., Guitton, D. & Pack, C. C., 2017. Coherent alpha oscillations link current and future receptive fields during saccades. *Proc. Natl. Acad. Sci. USA,* 114(29), pp. E5979-E5985.

Niv, Y. et al., 2015. Reinforcement learning in multi-dimensional environments relies on attention mechanisms. *J. Neurosci.,* 35(21), pp. 8145-8157.

O'Scalaidhe, S. P., Wilson, F. A. & Goldman-Rakic, P. S., 1999. Face-selective neurons during passive viewing and working memory peformance of rhesus monkeys: Evidence for intrinsic specialization of neuronal coding. *Cereb. Cortex,* 9(5), pp. 459-475.

Otero-Millan, J., Alba Castro, J. L., Macknik, S. L. & Martinez-Conde, S., 2014. Unsupervised clustering method to detect microsaccades. *J. Vis.,* 14(2), pp. 1-17.

Ott, T. & Nieder, A., 2019. Dopamine and cognitive control in prefrontal cortex. *Trends Cogn. Sci.,* 23(3), pp. 213-234.

Palva, S. & Palva, J., 2011. Functional roles of alpha-band phase synchronization in local and large-scale cortical networks. *Front. Psychol.,* Volume 2, p. 204.

Passingham, R. E., Toni, I. & Rushworth, M. F., 2000. Specialisation within the prefrontal cortex: the ventral prefrontal cortex and associative learning. In: W. X. Schenider, A. M. Owen & J. Duncan, eds. *Executive Control and the Frontal Lobe: Current Issues.* Berlin: Springer, pp. 103-113.

Pasupathy, A. & Miller, E. K., 2005. Different time courses of learning-related activity in the prefrontal cortex and striatum. *Nature,* Volume 433, pp. 873-876.

Paton, J. J., Belova, M. A., Morrison, S. E. & Salzman, D. C., 2006. The primate amygdala represents the positive and negative value of visual stimuli during learning. *Nature,* Volume 439, pp. 865-870.

Pesaran, B., 2008. Spectral analysis for neural signals. In: P. Mitra, ed. *Neural Signal Processing: Quantitative Analysis of Neural Activity.* Washington: Society for Neuroscience, pp. 1-12.

Pesaran, B., Hagan, M., Qiao, S. & Shewcraft, R., 2021. Multiregional communication and the channel modulation hypothesis. *Curr. Opin. Neurobiol.,* Volume 65, pp. in-press.

Pestilli, F., Carrasco, M., Heeger, D. J. & Gardner, J. L., 2011. Attentional enhancement via selection and pooling of early sensory responses in human visual cortex. *Neuron,* 72(5), pp. 832-846.

Petrov, A. A., Dosher, B. A. & Lu, Z.-L., 2005. The dynamics of perceptual learning: an incremental re-weighting model. *Psychol. Rev.,* 112(4), pp. 715-743.

Popescu, A. T., Popa, D. & Paré, D., 2009. Coherent gamma oscillations couple thje amygdala and striatum during learning. *Nat. Neurosci.,* Volume 12, pp. 801-807.

Puig, V. M. & Miller, E. K., 2012. The role of prefrontal dopamine D1 receptors in the neural mechanisms of associative learning. *Neuron,* 74(5), pp. 874-886.

Rajalingham, R. & Dicarlo, J. J., 2019. Reversible inactivation of different millimeter-scale regions of primate IT results in different patterns of core object recognition deficits. *Neuron,* 102(2), pp. 493-505.e5.

Ranganath, C., 2006. Working memory for visual objects: Complementary roles of inferior temporal, medial temporal, and prefrontal cortex. *Neuroscience,* 139(1), pp. 277-289.

Reingold, E. M. & Sheridan, H., 2011. Eye movements and visual expertise in chess and medicine. In: S. P. Liversedge, I. D. Gilchrist & S. Everling, eds. *The Oxford handbook of eye movements.* s.l.:Oxford University Press, pp. 523-550.

Roelfsema, P. R. & van Ooyen, A., 2005. Attention-gated reinforcement learning of internal representations for classification. *Neural Comput.,* 17(10), pp. 2176-2214.

Roelfsema, P. R., van Ooyen, A. & Watanabe, T., 2010. Perceptual learning rules based on reinforcers and attention. *Trends Cogn. Sci.,* 14(2), pp. 64-71.

Rolls, E. T. & Tovee, M. J., 1995. Sparseness of the neuronal representation of stimuli in the primate temporal visual cortex. *J. Neurophysiol.,* 73(2), pp. 713-726.

Rubin, N., Nakayama, K. & Shapley, R., 1997. Abrupt learning and retinal size specificity in illusory-contour perception. *Curr. Biol.,* 7(7), pp. 461-467.

Rubin, N., Nakayama, K. & Shapley, R., 2002. The role of insight in perceptual learning: evidence from illusory contour perception. In: M. Fahle & T. Poggio, eds. *Perceptual Learning.* s.l.:MIT Press, pp. 235-251.

Sakagami, M. & Pan, X., 2007. Functional role of the ventrolateral prefrontal cortex in decision making. *Curr. Opin. Neurobiol.,* 17(2), pp. 228-233.

Salazar, R. F., Dotson, N. M., Bressler, S. L. & Gray, C. M., 2012. Content-specific fronto-parietal synchronization during visual working memory. *Science,* 338(6110), pp. 1097-1100.

Santernecchi, E. et al., 2019. Gamma tACS over the temporal lobe increases the occurrence of Eureka! moments. *Sci. Rep.,* Volume 9:5778, pp. 1-12.

Schoups, A., Vogels, R., Qian, N. & Orban, G., 2001. Practising orientation identification improves orientation coding in V1 neurons. *Nature,* 412(6846), pp. 549-543.

Serences, J. T. & Kastner, S., 2014. A multi-level account of selective attention. In: A. C. Nobre & S. Kastner, eds. *The Oxford handbook of attention.* s.l.:Oxford University Press, pp. 76-104.

Shadmehr, R. & Holcomb, H. H., 1997. Neural correlates of motor memory consolidation. *Science,* 277(5327), pp. 821-825.

Shepard, R. N., 1967. Recognition memory for words, sentences, and pictures. *J. verbal learn. verbal behav.,* 6(1), pp. 156-163.

Sprugnoli, G. et al., 2017. Neural correlates of Eureka moment. *Intelligence,* Volume 62, pp. 99-118.

Standing, L., 1973. Learning 10000 pictures. *Q J Exp Psychol.,* 25(2), pp. 207-222.

Stanisor, L., van der Togt, C., Pennartz, C. M. & Roeflsema, P. R., 2013. A unified selection signal for attention and reward in primary visual cortex. *Proc. Natl. Acad. Sci. USA,* 110(22), pp. 9136-9141.

Tanaka, K., 1996. Inferotemporal cortex and object vision. *Annu. Rev. Neurosci.,* Volume 19, pp. 103-139.

Tanaka, K., Saito, H., Fukada, Y. & Moriya, M., 1991. Coding visual images of objects in the inferotemporal cortex of the macaque monkey. *J. Neurophysiol.,* 66(1), pp. 170-189.

Tort, A. B., Komorowski, R. W., Manns, J. R. & Kopell, N. J., 2009. Theta–gamma coupling increases during the learning of item–context associations. *Proc. Natl. Acad. Sci. USA,* 106(49), pp. 20942-20947.

Tovee, M. J., Rolls, E. T. & Ramachandran, V. S., 1996. Rapid visual learning in neurones of the prime temporal visual cortex. *Neuroreport,* 7(15-17), pp. 2757-2760.

Tse, D. et al., 2007. Schemas and memory consolidation. *Science,* 316(5821), pp. 76-82.

Tsunoda, K., Yamane, Y., Nishizaki, M. & Tanifuji, M., 2001. Complex objects are represented in macaque inferotemporal cortex by the combination of feature columns. *Nat. Neurosci.,* 4(8), pp. 832-838.

Van Kerkoerle, T. et al., 2014. Alpha and gamma oscillations characterize feedback and feedforward processing in monkey visual cortex. *Proc. Natl. Acad. Sci. USA,* 111(40), pp. 14332-41.

Verbeke, P., Ergo, K., De Loof, E. & Verguts, T., 2021. Learning to synchronize: Midfrontal theta dynamics during rule switching. *J. Neurosci.,* 41(7), pp. 1516-1528.

Walsh, V. & Booth, M., 1997. Perceptual learning: Insight in sight. *Curr. Biol.,* 7(4), pp. R249-R251.

Wang, Y. & Dragoi, V., 2015. Rapid learning in visual cortical networks. *eLife,* Volume 4:e08417, pp. 1-16.

Watanabe, K. & Hikosaka, O., 2005. Immediate changes in anticipatory activity of caudate neurons associated with reversal of position-reward contigency. *J. Neurophysiol.,* 94(3), pp. 1879-1887.

Watanabe, T. & Sasaki, Y., 2015. Perceptual learning: toward a comprehensive theory. *Annu. Rev. Psychol.,* Volume 66, pp. 197-211.
Williams, Z. M. & Eskander, E. N., 2006. Selective enhancement of associative learning by microstimulation of the anterior caudate. *Nat. Neurosci.,* Volume 9, pp. 562-568.
Yamins, D. L. & Dicarlo, J. j., 2016. Eight open questions in the computational modeling of higher sensory cortex. *Curr. Opin. Neurobiol.,* Volume 37, pp. 114-120.
Yang, T. & Maunsell, J. H., 2004. The effect of perceptual learning on neuronal response in monkey visual area V4. *J. Neurosci.,* 24(7), pp. 1617-1626.
Yao, H. et al., 2007. Rapid learning in cortical coding of visual scenes. *Nat. Neurosci.,* 10(6), pp. 772-728.
Zanos, T. et al., 2015. A sensorimotor role for traveling waves in primate visual cortex. *Neuron,* 85(3), pp. 615-627.
Zeitler, M., Fries, P. & Gielen, S., 2006. Assessing neuronal coherence with single-unit, multi-unit and local field potentials. *Neural Comput.,* 18(9), pp. 2256-2281.

STAR★Methods

KEY RESOURCES TABLE

REAGENT or RESOURCE	SOURCE	IDENTIFIER
Experimental Models: Organisms/Strains		
Rhesus macaque, Macaca mulatta (males, 4 and 10 years)	McGill University	N/A
Software and algorithms		
MATLAB R2016b	Mathworks	RRID:SCR_001622
Chronux	http://chronux.org (Mitra & Bokil, 2008)	v2.12.3
Microsaccade Detection	(Otero-Millan, et al., 2014)	N/A
3D Slicer	http://slicer.org (Fedorov, et al., 2012)	4.11
Other		
Utah multielectrode arrays	Blackrock Microsystems, Utah (USA)	Iridium Oxide, 96 Channel
Macaque Atlas (Figure 2)	(Markov, et al., 2014)	Core-Nets https://core-nets.org

RESOURCE AVAILABILITY

Lead Contact

Further information should be directed to and will be fulfilled by the Lead Contact, Bennett Csorba (bennett.csorba@mail.mcgill.ca).

Materials Availability

This study did not generate any unique materials.

Data and Code Availability

At the time of publishing, the behavioral and neural data will be available from the lead contact upon reasonable request.

Experimental Setup

Animal preparation

Two adult male rhesus macaque monkeys (*Macaca mulatta*, 4 and 10 years old) participated in the study. All animal care, surgical and experimental procedures were approved by the Montreal Neurological Institute's Animal Care Committee, and the animals were monitored by the veterinary staff for the duration of the experiment.

Experimental preparation has been described in a previous publication (Krause, et al., 2017). In brief, high-resolution T1 and T2-weighted anatomical MRIs (0.6-0.8 mm^3 voxels) were acquired for each animal and were used for surgical planning. Animals were implanted with a custom titanium head post (Hybex Innovations, Montreal Canada) using standard sterile surgical techniques. Post-recovery, animals were familiarized with the laboratory environment, and were trained for head fixation and subsequently the behavioral "foraging" task. Once overall performance in this paradigm was stable, we prepared the animals for electrophysiology.

A second surgery was then performed to implant multielectrode arrays into IT (area TEO) and the lateral PFC, ventral to the principal sulcus (area 46v). This part of PFC receives projections from IT and is often considered part of the machinery for visual image recognition (Kravitz, et al., 2013; Kar & DiCarlo, 2021). A neuro-navigation system (Brainsight Vet; Rogue Research Montreal Canada) synced with previously completed MRI scans was used to ensure that the arrays were accurately positioned. Arrays were then inserted into PFC and IT using a pneumatic device. The positions of the arrays were verified post-operatively (Figure 2), via coregistration of preoperative MRI scans with postoperative CT scans.

Behavioral tasks

Non-human primates were seated in front of a screen that spanned 30x60 degrees of visual angle, at a viewing distance of 40cm. Eye positions were sampled at 500 Hz with an infrared eye tracker (SR Research, Ontario). During each session, the animals completed the foraging task described below over the course of approximately 30 minutes, with each trial following the progression shown in Figure 1A. Foraging trials were alternated with brief trials involving a calibration task (see below), to ensure precise calibration of the eye tracker. The foraging

paradigm was adapted from a previous study which investigated associative learning in humans (Chukoskie, et al., 2013).

Each trial of the foraging task began with the appearance of a high-contrast fixation cross on a gray screen. Animals initiated the trial by fixating within 2 degrees of the fixation spot for 750–1000 ms, after which they were presented with a full-screen image. Images were chosen from collections of Creative-Commons and public domain photographs of natural images (flickr.com). Image presentation order was randomized within each session, and sessions consisted of 75 or 100 trials (depending on the animal) of each of the two images.

A 2° reward zone (RZ) was embedded into a random location in each image, and jittered a small amount on each trial, according to a bivariate normal distribution with a standard deviation of 1–4 degrees. This encouraged the subjects to learn the spatiotopic location of the RZ, rather than a specific set of saccade vectors. Upon image presentation, animals could freely search the image until they found the RZ or 15 (Monkey F) or 20 (Monkey M) seconds elapsed. If animals did not successfully find the RZ within that time, a high-contrast cue was shown at the RZ to guide their saccades into it. Once the animals had successfully maintained gaze position within the RZ for 100 ms, they received a juice reward and the trial ended.

Throughout our electrophysiological recordings, behavioral performance was stable (linear regression between session number and N_{50}, $R^2 = 0.04$, $p = 0.12$). In the main experiment, images were not repeated across sessions. We also conducted 19 long-term recall sessions, in which animals "foraged" in image-reward zone pairs that they had seen 3–128 days earlier. Behavioral performance during these sessions is described separately in the Results, but the data are not included in any of the electrophysiological analyses.

Eye calibration

Eye calibration was checked on interleaved trials in which the animals were shown a grey screen with a single small, high-contrast saccade target, randomly located at one of 9 (or 25) locations on a 3x3 (or 5x5) grid spanning the central 14 horizontal and vertical degrees on the monitor. Animals received a liquid reward for making a saccade to the target and maintaining their gaze on it for 750–1,250 ms.

Behavioral data analysis

Response modeling

In each session, response times (RTs) for all presentations of each image were extracted. RTs were then smoothed with a three-element median filter to exclude transient lapses in engagement. The resulting response time curves were well-described by sigmoid functions, so the data were fit to a model described by the equation:

$$S(n) = -\ Gain \times \frac{1}{1 + e^{-Slope+(n-N50)}} + (Gain + MinRT)$$

where $S(n)$ is the response time on the n-th presentation of a given image. The *Gain* parameter represents the magnitude of the performance improvement obtained through learning. The parameter *MinRT* reflects the animal's asymptotic performance, or the response time necessary to complete the task once the association had been completely learned.

Similarly, the N_{50} parameter indexes the trial number at which the response time reaches the halfway point between its initial value and its asymptotic value. This parameter therefore identifies the midpoint of the shift from a pre-learning phase to a post-learning phase (Figure 1B). The *Slope* reflects how quickly the response time shifted from its maximum to its minimum.

We excluded data from images in which the parameters of the sigmoid fits were inconsistent with reliable task performance. For example, images for which $N_{50} < 0$ were generally too noisy to be interpreted. Images for which the animal failed to learn the association were those in which N_{50} was greater than 100, *Gain* was less than 3 s, or *MinRT* was greater than 3 s. We verified that the excluded data reflected a lack of learning, in terms of the overall improvement in performance throughout the session, but we did not perform any selection based on the abruptness of learning.

Saccadic eye movements

Saccade onset and offset were estimated from the eye position traces based on eye velocity and acceleration (Cornelissen, et al., 2012), followed by manual review to make small corrections to onset/offset times and to discard false detections. Microsaccades were extracted using an unsupervised clustering method (Otero-Millan, et al., 2014).

Electrophysiological data analysis

In some experiments on the same animals, we examined the influence of transcranial direct current stimulation (tDCS) on neural activity and behavior. These data have been reported in a separate paper (Krause, et al., 2017) and were excluded from the analyses reported here.

Processing of raw data

Wideband neural signals were recorded using a neural interface processor (Ripple Neuro, Salt Lake City, Utah). Neural signals were sampled at 30,000 Hz and band-pass filtered between 0.3 and 7,500 Hz during acquisition. These data were post-processed offline to remove powerline and low-frequency movement artifacts, using the Chronux functions rmlinesc and locdetrend respectively. Next, the local field potentials (LFPs) were extracted with a fourth order Butterworth low-pass filter (F_c = 500 Hz) and re-sampled at 1 kHz.

Subsequent analysis was performed with the MATLAB signal processing package Chronux (v2.12.3) and custom-written MATLAB software. The LFPs were manually reviewed for quality. Sites were excluded from analysis on individual sessions when they had an exceptionally low signal-to-noise ratio (SNR < 3). An average of 89 out of 96 IT sites, (*SE*=0.33, > 92% of all sites) and 95 of 96 PFC sites (*SE*=0.12, > 98% of all sites) were available for analysis.

Trial epoch selection

Three epochs of interest (Figure 1A) were chosen from the data from each trial: a Scene Onset epoch (400ms following scene onset), a Reward epoch (400ms following reward onset), and a Foraging epoch (225ms to 100ms before the onset of the first saccade on each trial). We chose to limit the analysis of the Foraging epoch to the time just before the onset of the first saccade because the free-viewing paradigm rendered the Foraging epoch otherwise uncontrolled in

terms of eye movements and visual stimulation. In particular, eye movements can strongly influence LFP signals (Zanos, et al., 2015; Jutras, et al., 2013).

The epoch durations were chosen based on preliminary analyses (Figure 3), with the intention to identify regions of interest in time-frequency space. Other bands and window sizes around these event epochs were considered for all reported neurophysiological measures to avoid biasing the results. See Figure 3, Figure S3 and Figure S4 for other frequency bands, which showed no effect.

Calculation of spectral power

Within each epoch, we estimated the LFP power (Figure S6A-B). For a raw signal *x*, the LFP was analyzed as the time varying spectral power *P* for each frequency *f*, according to the squared norm of its time-frequency transformation *X*:

$$P_x(t,f) = |X(t,f)|^2$$

For both recording areas, we took the average power across all usable electrodes on each trial, within each trial epoch. For each trial epoch, a maximal trial value was determined, to which all other trial values were normalized. Learning epoch averages were then computed from the normalized values.

Synchronization

To quantify synchronization (Figures 3–5, Figure S1B, Figure S6C-D), we computed LFP-LFP coherence, which is a measure of the linear correlation between two signals in the frequency domain (Zeitler, et al., 2006; Harris & Gordon, 2015) and a commonly-used metric of synchronization (Harris & Gordon, 2015). Coherence is independent of absolute phase and is often thought of as the consistency across trials of the relative phase angles between two signals. We computed LFP-LFP coherence with multi-taper methods, using five tapers and a spectral resolution of 7.5 Hz (Babadi & Brown, 2004; Pesaran, 2008).

Session averages for LFP-LFP coherence (Figure 4) were computed by taking the median values across usable electrodes within (max. 4560 pairs each) or between (max. 9126 pairs) IT and PFC. Because coherence is not defined on a single trial, we used five-trial windows to compute coherence across trials throughout each session. This allowed us to capture relatively abrupt changes in the communication between IT and PFC that occurred over the course of a few trials. The first and last two trials of each session used three-trial and four-trial windows respectively to compute coherence, but these data were rarely used.

As with power, we normalized coherence values to the maximum values within each trial epoch. Normalization was done independently at each frequency. Averages within each learning epoch (Figure 3; Figure S1B) were then computed from the normalized trial values for each trial epoch.

Calculation of cross-correlations and lags

The lags between two band-filtered signals x_1 and x_2 were computed from the cross-correlation of the amplitudes of the Hilbert transformations of the two signals $H(x_1)$ and $H(x_2)$. Within individual sessions, cross-correlation values were computed between all usable electrodes on

every trial (for each trial epoch and for all bands). Time lags between IT and PFC were then extracted from the peak of their cross-correlations. Averages for each trial epoch were then computed within each session and averaged across sessions.

Multi-unit analysis

Because single-unit activity was generally sparse in both areas, we focused on multi-unit activity in this study. A three-step process was used to extract multi-unit activity from the wideband signals. First, the raw signals were high-pass filtered (F_c = 500 Hz), using a 3rd-order Butterworth filter. Multi-unit events were then defined as the instants where the resulting signal exceeded 3 robustly-estimated standard deviations from the mean (i.e., 4.2 median absolute deviations). To avoid double-counting events, we imposed a 2-ms refractory period immediately after each threshold crossing. We defined MUA responsiveness as the mean rate of MUA events (Figure 6) in units of events/s, occurring on each electrode during the 400 ms after the reward was dispensed ("reward responsiveness") or after scene onset ("image responsiveness").

We used a linear discriminant analysis (LDA) to identify subsets of electrodes whose multi-unit activity were more (or less) selective for the scenes being presented, and to determine if neuronal selectivity improved with learning. Classification was done independently for each experimental session, and classifiers were trained separately on IT activity and PFC activity using scene labels as class inputs (Figure 6). Two unique scenes were shown on every session, so the classifier was always trained to discriminate between two data classes. LDA classifiers were trained on multi-unit activity collected on all available electrodes in IT and PFC, using the responses obtained at each site during the scene onset epoch. We chose this epoch because it provided the purest measure of sensory selectivity, without confounding influences of eye movements or rewards.

Classification performance on individual sessions was computed using leave-one-out cross-validation. Because population selectivity did not change post-learning in either IT or PFC (Figure 6A), the classifiers were trained on all trials within a session. Classifiers were also trained on shuffled class data as a control, where the expected 50% baseline classification rate was observed. Classifiers consistently relied on different IT electrodes to classify images across sessions (Figure S2A) in both animals, as would be expected from the variable selectivity of different IT sites (Rajalingham & Dicarlo, 2019).

Statistics

Because the data set consists of data from two monkeys, we generally used permutative two-way ANOVAs (Corain & Salmaso, 2007) to ensure that all results were consistent between monkeys. When testing linear correlations between two groups, Pearson's *r* values were computed (Havlicek & Peterson, 1976).

All significance thresholds were corrected for multiple comparisons where necessary. Correcting for multiple comparisons was done by adjusting with a Holm-Bonferroni correction or a false discovery rate criterion (Benjamini & Yekutieli, 2005), depending on the correct context. All statistical tests were performed in MATLAB.